BNL-108272-2015-JA

Charge trapping and de-trapping in isolated CdSe/ZnS nanocrystals under an external electric field: indirect evidence for a permanent dipole moment

[1]Huidong Zang, [2]Mihail Cristea,[1] Xuan Shen,[1]Mingzhao Liu, [1]Fernando Camino and [1,*]Mircea Cotlet

[1]Center for Functional Nanomaterials, Brookhaven National Laboratory, Upton NY 11973, USA and [2]Physics Department, University "Politehnica" of Bucharest, 313 Splaiul Independentei, Bucharest RO-060042, Romania

Correspondence email: cotlet@bnl.gov

Abstract. Single nanoparticle studies of charge trapping and de-trapping in core/shell CdSe/ZnS nanocrystals incorporated in an insulating matrix and subjected to an external electric field demonstrate the ability to reversibly modulate the exciton dynamics and photoluminescence blinking while providing indirect evidence for the existence of a permanent ground state dipole moment in such nanocrystals. A model assuming the presence of energetically deep charge traps physically aligned along the direction of the permanent dipole is proposed in order to explain the dynamics of nanocrystal blinking in the presence of a permanent dipole moment.

Keywords: (colloidal quantum dots, charge transfer, dipole moment, blinking, quantum-confined Stark effect)

Colloidal semiconductor quantum dots (Qdots) have received increased attention due to their size-dependent optoelectronic properties and their potential utilization as light harvesting nanocrystals in photovoltaic solar cell and light emitting diode applications, as well as nanotags in biological imaging and sensing.[1-7] The intrinsic photophysical properties of various types of Qdots have been intensively studied, and in particular with single nanocrystal spectroscopy (SNS) methods.[8-15] However, the photophysical properties of Qdots subjected to an external electric field and in particular the behavior at single nanocrystal level, have received somehow sporadic attention.[16-20] A Qdot can interact with an external electric field in several ways. A Qdot can be placed in a capacitor-like geometry such as in a light emitting diode device, where the electric field is applied between two parallel electrodes,[7, 21] herein named external electric field. A Qdot can also interact with a localized intermolecular electric field generated by charge transfer/charge separation when coupled to a charge acceptor,[22, 23] like encountered in solar cells.[5, 24, 25] Charge carriers generated in or injected onto a Qdot core will sense such external electric fields. Therefore, investigation of the optical response of Qdots subjected to such electric fields is of fundamental importance in understanding and improving the performance of next generation nanocrystal-based optoelectronic devices.

Charge injection, charge trapping and de-trapping in isolated QDs have been extensively investigated with SNS methods[16, 26-33], in particular exciton dynamics and photoluminescence (PL) blinking. PL blinking, or reversible switching of emission of an isolated Qdot between bright (on-) and dark (off-) states when under continuous illumination has been discovered by Nirmal et al[9] and explained by the so called Auger recombination model which assumes charging of the photoexcited Qdot core due to electron ejection into long-lived traps followed by efficient Auger recombination which keeps the Qdot dark. Modified Auger recombination

models have since been proposed and they invoked the existence of a distribution of trap states, traps diffusing at the core/shell interface or fluctuating tunneling barriers for the ejected electron.[8, 34, 35] This model can explain Qdots featuring binary-like on/off signals (states) where a positive trion accounts for the off-state. However, Qdots can feature sometimes a three-state level PL blinking, with an additional dim (grey) state associated with emission from a negative trion[14, 15, 26, 30, 36]. SNS combined with electrochemistry demonstrated recently that dim emission is associated with the formation of negative trions[29, 30, 37]. SNS combined with an external electric field has been employed to demonstrate reversible modulation of the PL emission from Qdots and to assess the magnitude of the quantum confined Stark effect in Qdots.[16, 38, 39]

CdSe nanocrystals have been reported to possess a rather large permanent dipole both by theoretical and experimental studies[40-42], a property arising supposedly from their unique non-centrosymmetric, Wurtzite crystal structure. However, the presence of a permanent dipole in CdSe nanocrystals and its effect on the exciton dynamics and photoluminescence on/off blinking of such isolated Qdots has been so far neglected at best.

In this present work, we studied the external electric field effect on the PL intensity, PL lifetime and PL blinking and the QCSE for isolated CdSe/ZnS Qdots, demonstrated reversible changes in PL properties of isolated Qdots with alternating external electric field and provide a physical model that explains the observed PL changes with electric field and that takes into account a permanent dipole.

Results and Discussion

In our experiments, highly diluted CdSe/ZnS Qdots with PL emission at 605nm, core size of 4.4nm and shell thickness of 1.6nm (see Fig.S5, Supporting Information, SI) were sandwiched

between two insulating thin layers of silicon dioxide (SiO_2) and poly(methyl methacrylate) (PMMA), respectively, each layer 200 nm thick, and further sandwiched between two electrodes, Indium Tin Oxide (ITO) and Aluminum (Al) (Fig.1a). This type of architecture prevents charge injection onto Qdots and minimizes boundary conditions as both materials have similar value for the dielectric constant (3.9). A fluorescence-lifetime imaging microscopy (FLIM) image of isolated Qdots incorporated in the device and in the absence of an external electric field ($\vec{E} = 0$) and following 440nm excitation is presented in Fig.1b. Photon pair correlation (antibunching) experiments confirmed interrogation of isolated Qdots (see Fig.S1, SI). Figure 1c shows the PL intensity trajectory and PL lifetimes with the associated histograms from an isolated Qdot in the absence of external $\vec{E}$, with the classical on/off switching between bright and dark states. An external $\vec{E}$ applied to the device in the form of a triangular wave to the device (Fig.2a) modulates the PL intensity of isolated Qdots (Fig.2b), a behavior previously reported by others.[16, 39]

Herein we define forward bias, e.g. positive electric field ($+\vec{E}$), the field pointing from ITO to Al (Fig.1a). Accordingly, a Qdot under laser excitation and external $\vec{E}$ as that one shown in Fig.2b exhibits increase in PL intensity (black curve) with increase in external $\vec{E}$ pointing in forward configuration ($+\vec{E}$) and vice versa under reverse bias configuration ($-\vec{E}$), and so on. PL lifetimes from the same Qdot under external $\vec{E}$ follow similar modulation (Fig.2b, red dots), with PL intensity and PL lifetime exhibiting correlated behavior (Fig.2c).

Alternatively, a constant external $|\vec{E}|$ =0.5 MV/cm in either forward or reverse direction was applied to isolated Qdots to record their response with external $\vec{E}$. Figure 3 is such an example where the same Qdot is first probed without external $\vec{E}$ (zero bias, Fig.3a-c, black colored data), and found to emit with an average PL intensity of 8.8 kcounts/s (Fig.3a-b, black colored

data) and at an average PL lifetime of 19.7 ns (Fig.3c, black colored decay). Applying a reverse bias ($\vec{E}$ =-0.5MV/cm) increases both the PL intensity and PL lifetime, up to 9.5kCounts/s (Fig.3a-b, red colored data) and 21.1 ns (Fig.3c, red colored decay), respectively. Suppression of the external $\vec{E}$ returns the Qdot to the initial state since both the PL intensity (Fig.3d-e, black colored data) and the PL lifetime (Fig.3f, black colored decay) decrease to 9 kcounts/s and 18.8 ns, respectively. In a last step, applying a forward external $\vec{E}$ ($\vec{E}$=+0.5MV/cm) further suppresses the PL intensity (Fig.3d-e, red colored data) and PL lifetime (Fig.3f, red colored decay) of the same Qdot, now down to 7.5 kcounts/s and 16.9 ns, respectively.

Following these reversible demonstrations of PL modulation of in isolated Qdots by the use of either periodic (waveform, Fig.2) or constant but alternating bias (Fig.3), we next studied the statistical behavior of multiple isolated Qdots under a fixed external electric field, with about 60 isolated Qdots probed under reversed bias ($\vec{E}$=-0.5MV/cm). We studied and discuss herein in particular the effect of external $\vec{E}$ on the exciton dynamics (PL lifetime), PL blinking and QCSE in isolated Qdots. In the following discussion on the statistical behavior we consider only Qdots that exhibited response (changes in PL intensity and PL lifetimes) under reversed bias ($-\vec{E}$). According to Fig.4, from the isolated Qdots that were responding to external $\vec{E}$, 55% exhibited a decrease in PL lifetime, (Fig.4a, red vs green colored data), on average from 24.3 ns to 20.6 ns and accompanied by a decrease in PL intensity. The rest of Qdots (45%) showed an increase in PL lifetime (Fig.4b, red vs green colored), from 24.7 ns to 27.8 ns, accompanied by an increase in PL intensity. We categorize Qdots according to their response to the external -$\vec{E}$ in group A (QD(A)) which includes those Qdots exhibiting decrease in PL intensity/PL lifetime with reverse bias and in group B (QD(B)) which includes Qdots exhibiting increase in their PL lifetimes/PL intensity, respectively (Figs. 4a&b).

Figure 5 displays "ensemble-like" probability distributions for the on-state ($P(t_{on})$) and off-state ($P(t_{off})$) for group QD(A) (Fig.5a-c) and group QD(B) (Fig.5b-d) Qdots, respectively. Each probability includes events from all Qdots associated with a group, with each Qdot interrogated for 60 seconds. Each probability was built with on- and off-times estimated from PL traces like those shown in Fig.1a with a threshold method and fitted by a power-law model $P(t) = a \times t^{-m}$,[8] with m a power law exponent, and the results in Table 1 show that the two groups respond differently to the external $-\vec{E}$: group QD(A) exhibits clear decrease in on-time (increase in m_{on}), while group QD(B) exhibits clear increase in on time (decrease in m_{on}) with applied $-\vec{E}$. This same blinking bias trend with external electric field is observed even for the P (t_{on}) distributions built with data from the same single QD and for different bin times used to build such distributions, confirming the observed trend is real (see Fig.S2, SI)[43]. P (t_{off}) distributions on the other hand do not show clear changes in off-time (m_{off}) for both groups (Figs.5c,d).

Among various blinking models it is widely accepted that charge carrier traps play an important role in regulating the PL emission from Qdots.[8, 9, 34-36] Traps are energetically favorable defects located usually at the core/shell interface and capable of accepting photogenerated charge carriers from the Qdot's core. Passivation of Qdots reduces the number of surface traps and improves the PL quantum yield of Qdots.[44-46] In the assumption of a charge transfer process between the Qdot core and the trap, the PL lifetime of a Qdot can be written *a*s:

$$\tau_{PL} = \frac{1}{k_r + k_{nr} + k_{ct}} \quad (1)$$

with k_r, k_{nr} radiative and non-radiative rates and k_{ct} rate for charge transfer from the Qdot core to the trap site. An external $\vec{E}$ will affect the driving force for charge transfer from the

photoexcited core to the trap, which in turn will change k_{ct}: if k_{ct} increases under applied external $\vec{E}$ (compared to zero bias), the PL lifetime will decrease in accordance to eq.(1), and this is what we observed for group QD(A). Conversely, when k_{ct} decreases under applied external $\vec{E}$ (from zero bias), the PL lifetime will increase, as observed for group QD(B). If trap sites were to be uniformly distributed around the Qdot's core surface, an external electric field would inevitably increase k_{ct} and thus would always decrease the PL lifetime as well as the "on-time" probability of blinking, regardless in which direction the external electric field is applied with respect to the Qdot. However, we find from Figs.4&5 that Qdots responding to external electric field show both increase and decrease in PL lifetimes and in "on –time" probabilities, which suggests the presence of a permanent dipole in Qdots interfering with the external $\vec{E}$ (see below). An external $\vec{E}$ can also affect k_r through the QCSE, and previous studies indicated the existence of QCSE in quantum wells and/or nanocrystals in external electric field.[38, 47-54] For the Qdots investigated here, due to their small core size (<50Å), QCSE can play a role in affecting the dynamics of the excited states. From a physical perspective, when a photogenerated electron-hole pair occurs inside the Qdot core, an external $\vec{E}$ applied to the Qdot can lead to two outcomes: (i) under external $\vec{E}$ the electron and hole states will shift to lower and higher energies, respectively, to decrease the total energy, leading to a red shift of the PL emission, independent on the direction of the external $\vec{E}$ (forward or reverse); (ii) an external $\vec{E}$ can separate the electron and hole to opposite direction inside the core, decreasing the wave-function overlap and consequently decreasing the electron-hole pair recombination efficiency or the radiative rate k_r , thus leading to a decrease in the Qdot's PL quantum yield, and an increase in PL lifetime according to eq.(1). Due to the existence of thermal excitations and local potential fluctuations, a Stark effect is hard to be observed at room temperature using conventional PL spectroscopy.[38] To overcome this

obstacle, we designed a two-color detection SNS experiment (detailed in SI) where the PL emission of an isolated Qdot was split into two spectral regions by the use of a dichroic mirror centered at 605 nm, e.g. the PL peak of Qdots in the absence of external $\vec{E}$ (Fig.6g, channels 1 and 2 depicted in red and blue, respectively). Therefore, by detecting the two spectral regions by identical single photon counting detectors, any PL spectral shift was sensed as a change in the ratio of the PL intensities of the red (channel 1) and blue spectral regions (channel 2). Fig.6 depicts two typical examples of Qdotss subjected to the same external $\vec{E}$, a triangular wave bias, that responded oppositely, showing behavior associated with either group QD(A) (Fig.6b,c) or group QD(B) (Fig.6e,f). Namely, the Qdot part of group QD(A) showed a decrease in PL intensity (Fig.6b) and a red shift in the PL spectrum (Fig.6c) with applied reverse bias (0 to -0.5 MV/cm), while the Qdot part of group QD(B) showed an increase in PL intensity (Fig.6e) and a blue shift of the PL spectrum (Fig.6f), also with applied reverse bias. The observation of both red and blue shift of the PL spectrum is another indication of the presence of a permanent intrinsic dipole moment in the investigated Qdots: with no permanent dipole, Qdots would otherwise should only exhibit a red shift of the PL spectrum in any conditions of bias and as discussed above. Based on the ratio changes between red and blue channels from Fig.6g, we obtained a dependency PL emission peak vs external electric field as shown in Fig.6h which features a red shift of about 3nm for a swipe from 0 to -0.5MV/cm (see Fig.S3, SI for details on derivation of Fig.6h). This small shift observed here for CdSe/ZnS Qdots is consistent with results published previously for type II CdTe/CdSe Qdots.[38] This red spectral shift is associated with a decrease in PL lifetime which contradicts eq.(1) when assuming a dominating QCSE. Indeed, in the hypothesis of strong QCSE, a red shift should be the result of a decrease in radiative rate due to a decrease in wave function overlap, and consequently accompanied by an increase in PL lifetime according to eq(1). Consequently, QCSE is not the primary drive for the observed modulation in the PL

intensity/PL lifetime of isolated Qdots under external $\vec{E}$. Rather we need to consider that changes in k_{ct} are due to the presence of an intrinsic permanent dipole (see below).

The existence of a permanent dipole moment for CdSe Qdots has been predicted theoretically[41, 55] and confirmed experimentally by dielectric dispersion spectroscopy[40]. It is believed that an internal dipole moment results from the intrinsic, wurtzite-like crystal structure of non-centrosymmetric nature (e.g. lacking inversion symmetry) of CdSe, where the shift of the Cd and Se planes inevitably leads to the formation of a permanent ground state dipole moment in its c-axis direction. We confirmed by high resolution TEM that Qdots probed by us are indeed of wurtzite-like crystal structure (see details in SI, Fig.S4).

One possible model to explain PL blinking in CdSe/ZnS Qdots in the presence of a permanent dipole moment is schematically depicted in Fig.7. Here a core/shell CdSe/ZnS Qdot embedded in a device and with charge traps is schematically represented by a three-energy level system. In this model, a photogenerated exciton in the Qdot core creates a hole in valance band (VB) and an electron in the conduction band (CB), which can recombine radiatively to emit a photon of lesser energy, or recombine non-radiatively by releasing the resulting energy as vibrations to the lattice. An electron from CB can also jump to the trap state leaving a hole in the core, with the Qdot now being positively charged and non-emissive (dark) due to efficient Auger recombination via trion formation.[9, 30, 31, 36] The trapped electron can recombine with the hole in the Qdot core, thus neutralizing the core, or it can transfer back to the CB. However, back electron transfer is unlikely in a type I band alignment as is the case of a CdSe/ZnS Qdot (Fig.7). Therefore, the binary on/off switching of the PL emission of a Qdot must result from repeated ionization/neutralization of the core and it has to be related to the existence of charge traps. Due to the large surface to volume ratio for a core/shell CdSe/ZnS Qdot, one expects that such defects are distributed around the core, at the

core/shell interface, leading to an energetically broad distribution of trap states around the core. Thus, the presence of a large intrinsic permanent dipole moment of about 70 Debye along the nanocrystal's *c*-axis of the wurtzite crystal structure[42] can generate an internal electric field in this same *c*-axis. This can bias the energy depth of the trap states, making those traps oriented parallel to the direction of the permanent dipole moment energetically favorable compared to traps aligned with the *a*- and *b*-axis of the wurtzite crystal structure (Fig.7). When an external electric field is applied to a Qdot, the relative direction of the internal electric field generated by the permanent dipole moment and the external applied electric field dictate the overall effect of the external electric field on the PL emitted by the Qdot: the external electric field can either increase or decrease the local electric field strength experienced by the charge carriers in the trap states. If the Qdot has a permanent dipole moment (projection in x-axis, Fig.7) aligned antiparallel to the external electric field applied in the device, an electron will be trapped easier (increased k_{ct}) and it will be kept longer in the trap state, a manifestation seen as a decrease in PL blinking on-time probability (increase of m_{on}) such as observed here for Qdots belonging to group QD(A) (Table 1). Consequently, group QD(B) will include Qdots with a permanent dipole moment (projection in x-axis) aligned parallel with the external electric field in the device and exhibiting increase in on-time blinking (decrease in m_{on}, Table 1). Qdots non-responsive to the external electric field will have a permanent dipole moment aligned rather off with the direction of the external electric field, that is, with an insignificant projection in the x-axis.

To confirm our proposed model invoking a permanent dipole moment in Qdots and possible resulting from the Wurtzite-like crystal structure, we performed theoretical simulations in which we calculated the overlap of electron and hole probability density distributions in a Qdot. Fig.8a shows the electron and hole probability density distributions without a

permanent dipole moment and under different external electric field strength, where the highest overlap is observed at z=0nm for $E = 0\ \mathrm{MV/cm}$. When an external electric field ($E = \pm 0.5\mathrm{MV/cm}$) is applied, the electron and hole probability density distributions separate from each other, which inevitably translates into a lower energy for the QD and therefore a red shift in PL spectrum. Next we performed calculations assuming a permanent dipole moment interacting with an external electric field either in parallel or antiparallel direction (Fig.8b). Our results show that the overlap of the probability density distribution between the electron and hole depends on the mutual direction of the external electric field and dipole moment vectors. For an external electric field parallel to the dipole moment the integral is smaller than for the case of zero external electric field, while the integral becomes larger for an external electric field oriented antiparallel to the dipole moment. Thus, both blue and red PL spectra shifts can only be explained by accepting the existence of a permanent dipole moment in the QCSE model, an observation consistent with our experimental data shown in Fig.6h, in which both blue and red PL spectra shift are observed.

Alternatives to a permanent dipole moment generated by the unique wurtzite structure of CdS have been proposed. For example, Park et al. proposed a blinking model invoking a transient internal dipole moment originating from deeply trapped charges at the core/shell interface or outer shell surface[16]. In that model, blinking will proceed with shallow traps located at the core/shell interface and in the electric field generated by deep traps. That model however assumes not interacting deep and shallow traps, while one would expect deep traps to dominate over shallow traps in extracting photogenerated charges from the Qdot core. Surface charges might also be the origin of permanent dipole moments in some nanocrystals, as proposed by Shim et for ZnSe nanocrystals[42] with a Zinc blende, centrosymetric structure. Finally, heterogeneity in nanocrystal shape as observed in the TEM data (SI, Fig.S6) might

play a role in the response of the isolated Qdots investigated here with applied bias and might account for the differences in the observed power law exponents for QDs under zero bias (Table 1).

Conclusion

In summary, we demonstrated the ability to reversibly switch the PL emitted by a colloidal Qdot with an external electric field and provided a blinking model that explains the observed behavior and takes into account a permanent dipole moment of the Qdot. We performed optical and electric experiments to assign the rather small contribution of QCSE in CdSe/ZnS Qdots exposed to an external electric field. We found that in order to explain the observed changes in exciton dynamics and PL blinking in Qdots under external electric field we need to invoke the presence of an intrinsic permanent dipole, previously suggested both by theory and experiment[40, 41, 55] and most probably originating from the wurtzite-like structure of CdSe Qdots. In view of a large intrinsic dipole moment and depending on its orientation with respect to the external applied electric field, a Qdot might enhance or inhibit its PL emission, as shown here by us by the observation of changes in PL lifetimes and PL blinking dynamics. As a result, for the probed Qdots responsive to the external electric field (74% of the total probed population), half of them exhibit PL intensity and PL lifetime decrease, while the rest show an opposite behavior. As such, our studies provide a strong, while indirect, evidence for the presence of an intrinsic dipole moment in CdSe/ZnS QDs. As such, a model including the presence of a deep trap with preferential orientation along the permanent dipole (along QD's *c*-axis) is proposed to explain changes in exciton dynamics, PL blinking and PL spectroscopy of isolated QDs under external electric field. Our proposed model is consistent with our previous findings that a deep trap in the form of an external electron acceptor can regulate PL blinking in CdSe/ZnS QDs[22]

Supporting Information

Supporting Information includes photon pair correlation experiments, details on materials and device fabrication procedures, details on time-resolved confocal PL microscopy including two-color detection, PL blinking data analysis, examples of on- time distributions for single QDs with varying bin time, high resolution TEM and QDs size distribution, error analysis of PL lifetimes and theoretical simulation of electron and hole's density probability distribution under the exist of both external electric field and intrinsic dipole moment.

Acknowledgements

Research carried out at in part at the Center for Functional Nanomaterials, Brookhaven National Laboratory and supported by the U.S. Department of Energy, Office of Basic Energy Sciences, by Contract No. DE-SC0012704. We would like to thank Dr. Qingping Meng of BNL for fruitful discussions on the work presented herein.

References

1. H. Mattoussi, G. Palui and H. B. Na, *Advanced Drug Delivery Reviews*, 2012, 64, 138-166.
2. I. L. Medintz, H. T. Uyeda, E. R. Goldman and H. Mattoussi, *Nature Materials*, 2005, 4, 435-446.
3. W. K. Leutwyler, S. L. Bürgi and H. Burgl, *Science*, 1996, 271, 933.
4. D. L. Klein, R. Roth, A. K. Lim, A. P. Alivisatos and P. L. McEuen, *Nature*, 1997, 389, 699-701.
5. W. U. Huynh, J. J. Dittmer and A. P. Alivisatos, *Science*, 2002, 295, 2425-2427.
6. S. Ren, L.-Y. Chang, S.-K. Lim, J. Zhao, M. Smith, N. Zhao, V. Bulović, M. Bawendi and S. Gradečak, *Nano Letters*, 2011, 11, 3998-4002.
7. H. Mattoussi, L. H. Radzilowski, B. O. Dabbousi, E. L. Thomas, M. G. Bawendi and M. F. Rubner, *Journal of Applied Physics*, 1998, 83, 7965-7974.
8. M. Kuno, D. P. Fromm, H. F. Hamann, A. Gallagher and D. J. Nesbitt, *J Chem Phys*, 2001, 115, 1028-1040.
9. M. Nirmal, B. Dabbousi, M. Bawendi, J. Macklin, J. Trautman, T. Harris and L. Brus, *Nature*, 1996, 383, 802-804.
10. D. Patra, I. Gregor, J. Enderlein and M. Sauer, *Applied Physics Letters*, 2005, 87.
11. S. E. Yalcin, J. A. Labastide, D. L. Sowle and M. D. Barnes, *Nano Letters*, 2011, 11, 4425-4430.
12. J. J. Peterson and D. J. Nesbitt, *Nano Letters*, 2009, 9, 338-345.
13. O. Schwartz, R. Tenne, J. M. Levitt, Z. Deutsch, S. Itzhakov and D. Oron, *ACS Nano*, 2012, 6, 8778-8782.
14. A. V. Malko, Y. S. Park, S. Sampat, C. Galland, J. Vela, Y. F. Chen, J. A. Hollingsworth, V. I. Klimov and H. Htoon, *Nano Letters*, 2011, 11, 5213-5218.

15. K. Zhang, H. Y. Chang, A. H. Fu, A. P. Alivisatos and H. Yang, *Nano Letters*, 2006, 6, 843-847.
16. S.-J. Park, S. Link, W. L. Miller, A. Gesquiere and P. F. Barbara, *Chemical Physics*, 2007, 341, 169-174.
17. E. Rothenberg, M. Kazes, E. Shaviv and U. Banin, *Nano Letters*, 2005, 5, 1581-1586.
18. S. Liu, N. J. Borys, J. Huang, D. V. Talapin and J. M. Lupton, *Physical Review B*, 2012, 86, 045303.
19. T. Chiba, J. Qi, H. Fujiwara and K. Sasaki, *The Journal of Physical Chemistry C*, 2012, 117, 2507-2510.
20. F. Vietmeyer, T. Tchelidze, V. Tsou, B. Janko and M. Kuno, *ACS nano*, 2012, 6, 9133-9140.
21. S. Coe, W.-K. Woo, V. B. Moungi Bawendi and cacute, *Nature*, 2002, 420, 800-803.
22. Z. Xu, Cotlet, M, *Small*, 2012, 8, 253-258.
23. Z. H. Xu and M. Cotlet, *Angew Chem Int Edit*, 2011, 50, 6079-6083.
24. S. A. McDonald, G. Konstantatos, S. Zhang, P. W. Cyr, E. J. Klem, L. Levina and E. H. Sargent, *Nat Mater*, 2005, 4, 138-142.
25. P. V. Kamat, *The Journal of Physical Chemistry C*, 2008, 112, 18737-18753.
26. C. Galland, Y. Ghosh, A. Steinbrueck, M. Sykora, J. A. Hollingsworth, V. I. Klimov and H. Htoon, *Nature*, 2011, 479, 203-U275.
27. A. L. Weaver and D. R. Gamelin, *Journal of the American Chemical Society*, 2012, 134, 6819-6825.
28. V. Biju, M. Micic, D. Hu and H. P. Lu, *Journal of the American Chemical Society*, 2004, 126, 9374-9381.
29. W. Qin, R. A. Shah and P. Guyot-Sionnest, *ACS Nano*, 2012, 6, 912-918.
30. P. P. Jha and P. Guyot-Sionnest, *ACS Nano*, 2009, 3, 1011-1015.
31. W. Qin and P. Guyot-Sionnest, *ACS Nano*, 2012, 6, 9125-9132.
32. H.-S. Chen, T.-H. Chung, M.-C. Lin, Y.-W. Lan, C.-D. Chen and H.-Y. Lin, *Opt. Express*, 2010, 18, 26872-26878.
33. H. Huang, A. Dorn, G. P. Nair, V. Bulović and M. G. Bawendi, *Nano Letters*, 2007, 7, 3781-3786.
34. R. Verberk, A. M. van Oijen and M. Orrit, *Physical Review B*, 2002, 66.
35. J. Tang and R. A. Marcus, *Physical Review Letters*, 2005, 95.
36. D. E. Gomez, J. van Embden, P. Mulvaney, M. J. Fernee and H. Rubinsztein-Dunlop, *ACS nano*, 2009, 3, 2281-2287.
37. C. Galland, Y. Ghosh, A. Steinbrück, J. A. Hollingsworth, H. Htoon and V. I. Klimov, *Nature communications*, 2012, 3, 908.
38. K. Park, Z. Deutsch, J. J. Li, D. Oron and S. Weiss, *ACS nano*, 2012, 6, 10013-10023.
39. S. J. LeBlanc, M. R. McClanahan, T. Moyer, M. Jones and P. J. Moyer, *Journal of Applied Physics*, 2014, 115.
40. S. A. Blanton, R. L. Leheny, M. A. Hines and P. Guyot-Sionnest, *Physical Review Letters*, 1997, 79, 865-868.
41. E. Rabani, *The Journal of Chemical Physics*, 2001, 115, 1493-1497.
42. M. Shim and P. Guyot-Sionnest, *The Journal of Chemical Physics*, 1999, 111, 6955-6964.
43. C. H. Crouch, O. Sauter, X. H. Wu, R. Purcell, C. Querner, M. Drndic and M. Pelton, *Nano Letters*, 2010, 10, 1692-1698.
44. J. Antelman, Y. Ebenstein, T. Dertinger, X. Michalet and S. Weiss, *Journal of Physical Chemistry C*, 2009, 113, 11541-11545.
45. Y. Chen, J. Vela, H. Htoon, J. L. Casson, D. J. Werder, D. A. Bussian, V. I. Klimov and J. A. Hollingsworth, *Journal of the American Chemical Society*, 2008, 130, 5026-+.
46. P. Guyot-Sionnest, *Comptes Rendus Physique*, 2008, 9, 777-787.
47. D. Miller, D. Chemla, T. Damen, A. Gossard, W. Wiegmann, T. Wood and C. Burrus, *Physical Review Letters*, 1984, 53, 2173.

48. S. Empedocles and M. Bawendi, *Science*, 1997, 278, 2114-2117.
49. J. Mueller, J. M. Lupton, A. L. Rogach, J. Feldmann, D. V. Talapin and H. Weller, Baltimore, Maryland, 2005.
50. N. Yaacobi-Gross, N. Garphunkin, O. Solomeshch, A. Vaneski, A. S. Susha, A. L. Rogach and N. Tessler, *ACS nano*, 2012, 6, 3128-3133.
51. J. Seufert, M. Obert, M. Scheibner, N. A. Gippius, G. Bacher, A. Forchel, T. Passow, K. Leonardi and D. Hommel, *Applied Physics Letters*, 2001, 79, 1033-1035.
52. G. W. Wen, J. Y. Lin, H. X. Jiang and Z. Chen, *Physical Review B*, 1995, 52, 5913-5922.
53. L. Vina, E. Mendez, W. Wang, L. Chang and L. Esaki, *Journal of Physics C: Solid State Physics*, 1987, 20, 2803.
54. L. Vina, M. Potemski, J. Maan, G. Bauer, E. Mendez and W. Wang, *Superlattices and Microstructures*, 1989, 5, 371-374.
55. E. Rabani, B. Hetenyi, B. J. Berne and L. E. Brus, *The Journal of chemical physics*, 1999, 110, 5355-5369.

Figures and Figure captions

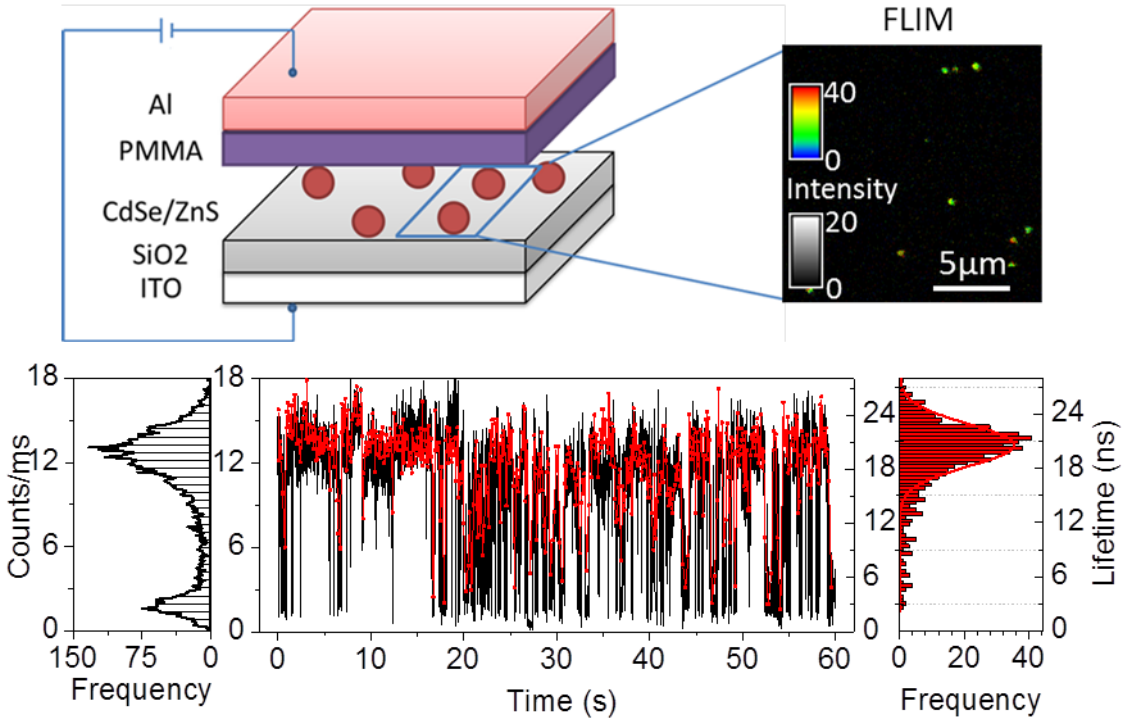

Figure 1. (a) Capacitor-like device architecture with highly diluted CdSe/ZnS QDs sandwiched between insulating PMMA and SiO_2 and with the bilayer structure sandwiched between ITO and Al electrodes. (b) FLIM image of isolated QDs in device in absence of external $\vec{E}$. (c) Time trajectories of PL intensity (black line) and PL lifetime (red line and squares) for an isolated QD (middle panel) in the absence of external $\vec{E}$, PL intensity histogram and PL lifetime histogram are shown in the left and right panel, respectively.

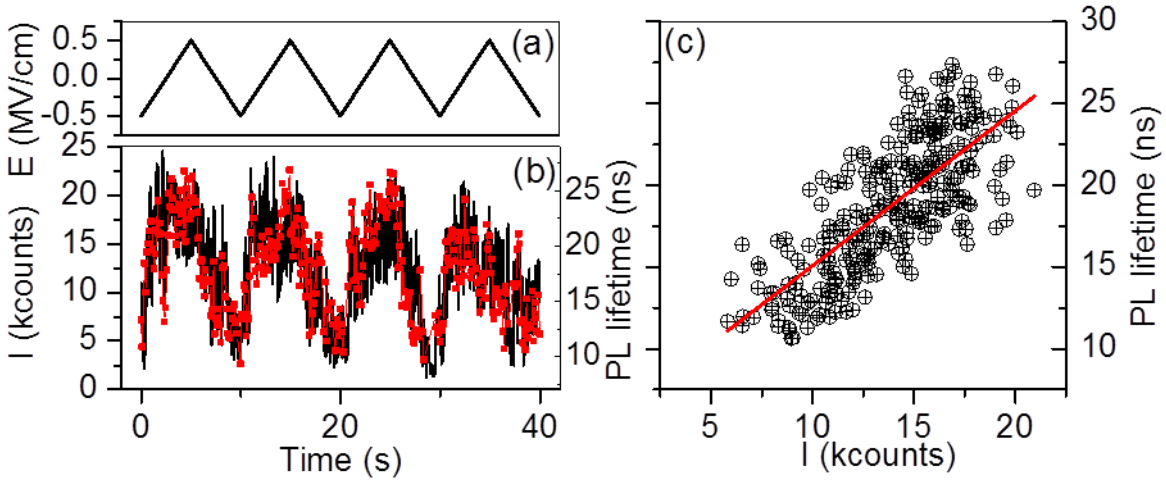

Figure 2.(a) External $\vec{E}$ is applied across the device containing QDs (Fig.1) as a triangular wave voltage signal with a periodicity of 10s; (b) PL intensity trajectory (black, 15ms dwell time) and associated PL lifetime trajectory (red squares and line) (dwell time 100 ms) from an isolated QD incorporated in device and under variable external $\vec{E}$; (c) PL intensity vs PL lifetime correlogram from the QD accounting for panel (b); PL intensity and lifetime data correspond to a dwell time of 117ms. Also shown is a linear fit of the correlogram.

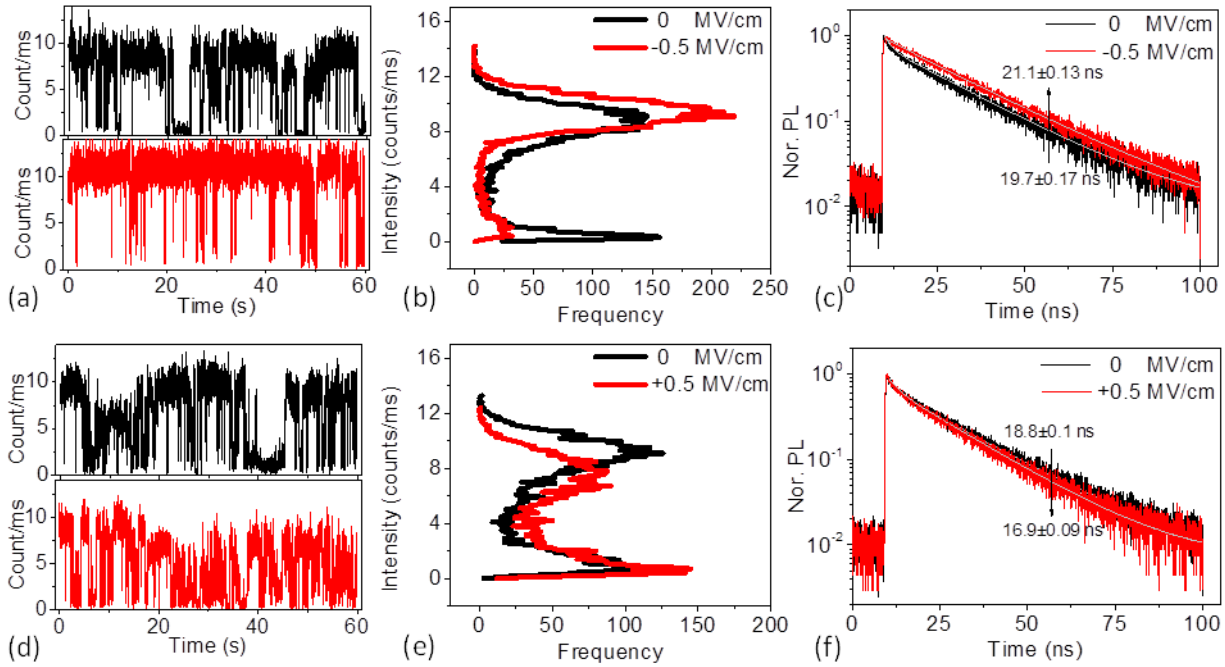

Figure 3. (a) PL intensity trajectories and (c) PL decays from an isolated QD subjected to zero electric bias (black traces) and then to reverse electric bias (red traces). The same isolated QD is further subjected back to zero electric bias (black) and forward electric bias (red) to record PL intensity trajectories, histograms and PL decays. Solid gray lines in (c) and (f) are bi-exponential fits and reported PL lifetimes are amplitude averaged. Panels (b) and (e) are color coded histograms of PL traces from panels (a) and (d).

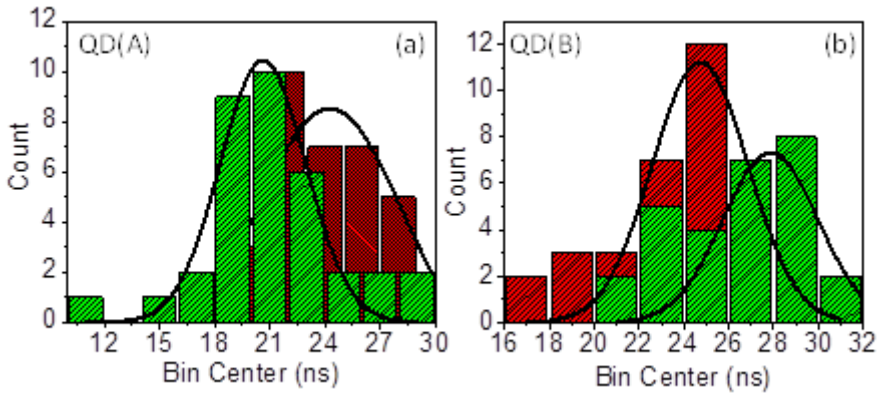

Figure 4. Histograms of PL lifetimes from isolated QDs under reverse bias ($-\vec{E}$) (green bars) and under zero bias (red bars) for (a) group and QD(A) and (b) group QD(B) nanocrystals. Black curves are Gauss fits showing, on average, decrease in PL lifetimes decrease from 24.3ns to 20.6ns for group QD(A) and increase from 24.7ns (red) to 27.8ns (green) for group QD(B).

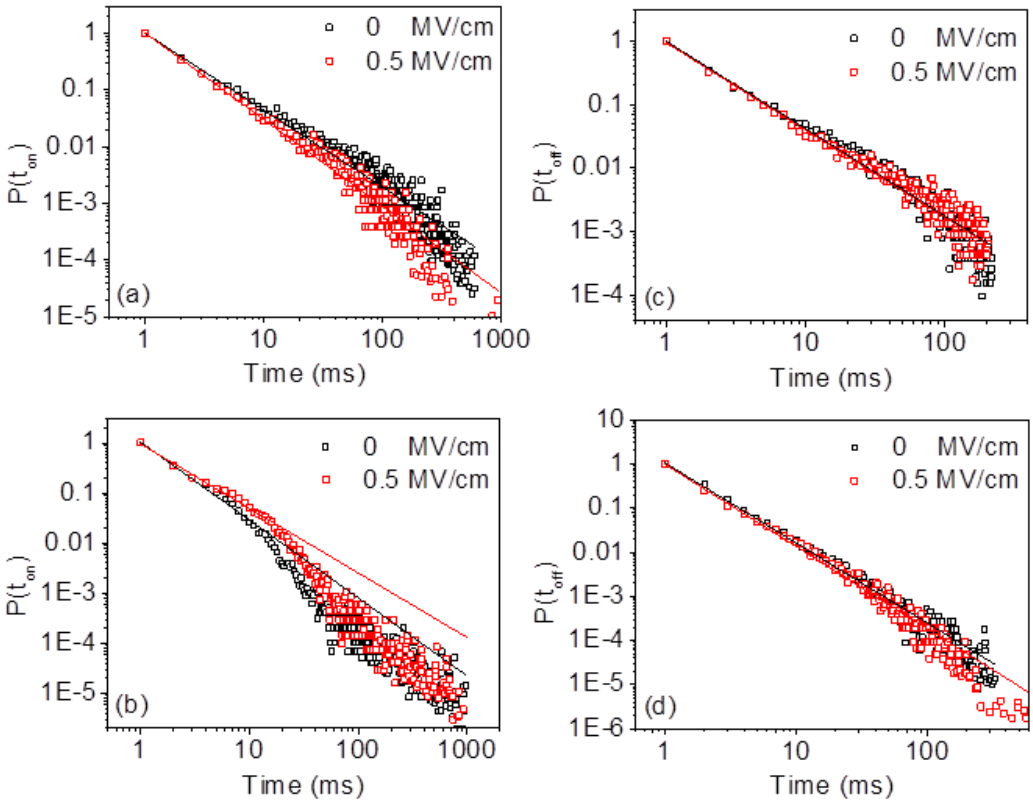

Figure 5. Probability distributions for on-times, $P(t_{on})$, (a-b), and of off-times, $P(t_{off})$, (c-d) for isolated QDs belonging to groups QD(A) (left panel) and QD(B) (right panel) under zero electric bias (black open squares) and under reverse external electric bias (red open squares). Fits according to a power law model are shown in solid lines and colored accordingly.

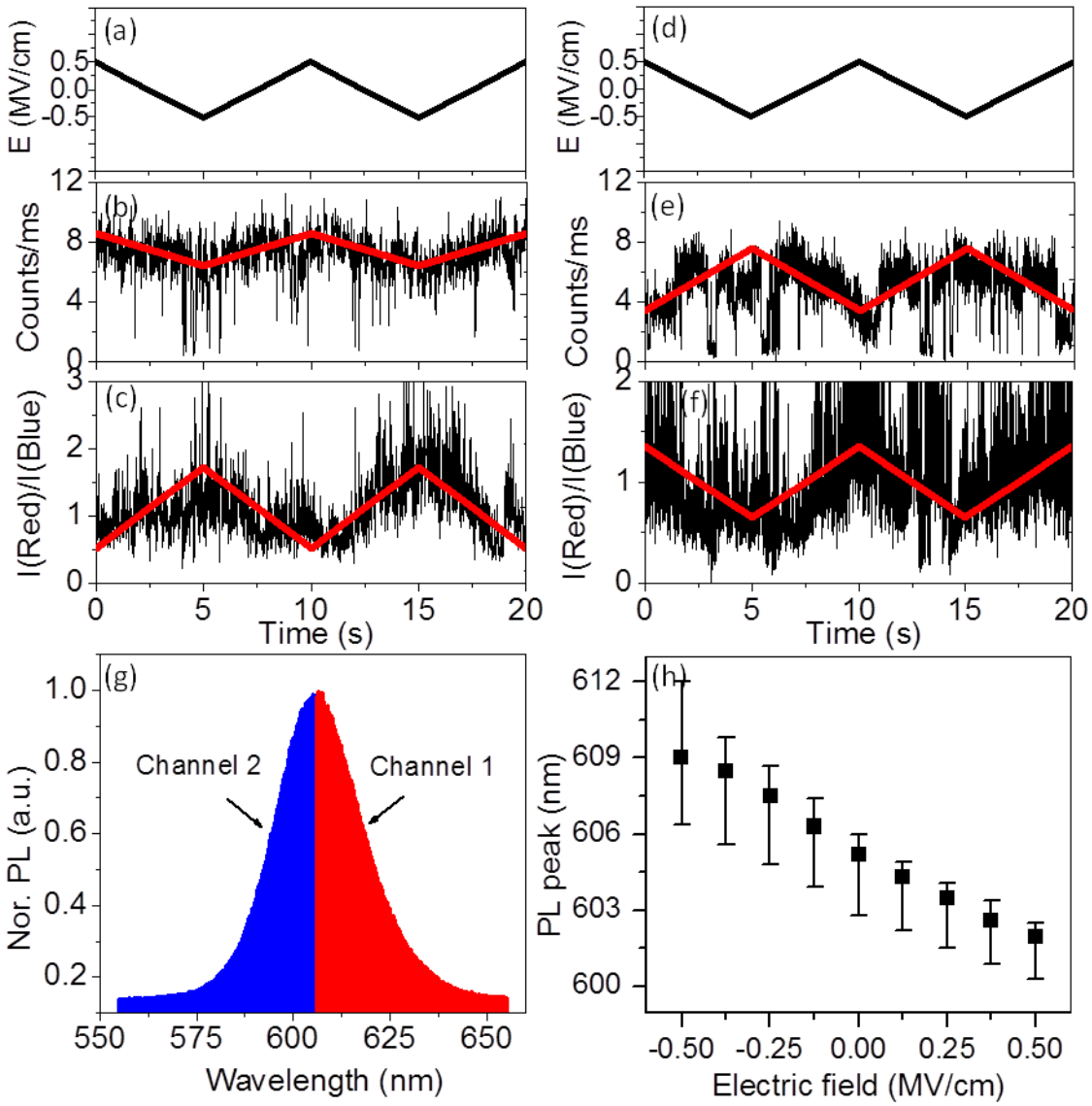

Figure 6.Two isolated QDs under identical external electric field show opposite behavior in PL response: (b-c) a QD part of group QD(A) exhibiting decrease in PL intensity (panel b) and red shift in PL emission (panel c) with increased reverse bias (panel a); (e-f) a QD part of group QD(B) exhibiting increase in PL intensity (panel e) and blue shift in PL emission under

reverse bias (panel f). (g) Normalized QD PL spectrum from bulk sample in solution features a full width at half maximum of 26nm; Red (channel 1) and blue (channels 2) spectral ranges used for deriving the ration I(red)/I(blue) data in panels (c) and (f). (h) Calculated PL spectral peak shift under external electric field for the QD(A) example from panel (c).

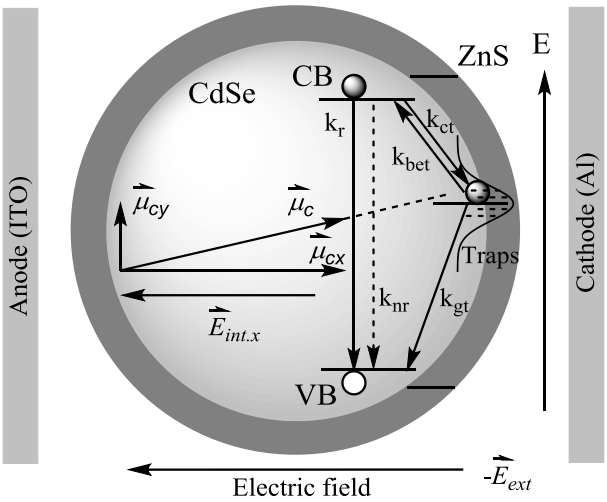

Figure 7. Schematic diagram of a QD located inside a device depicted with its two parallel electrodes. The trap site is located near cathode in this particular case.

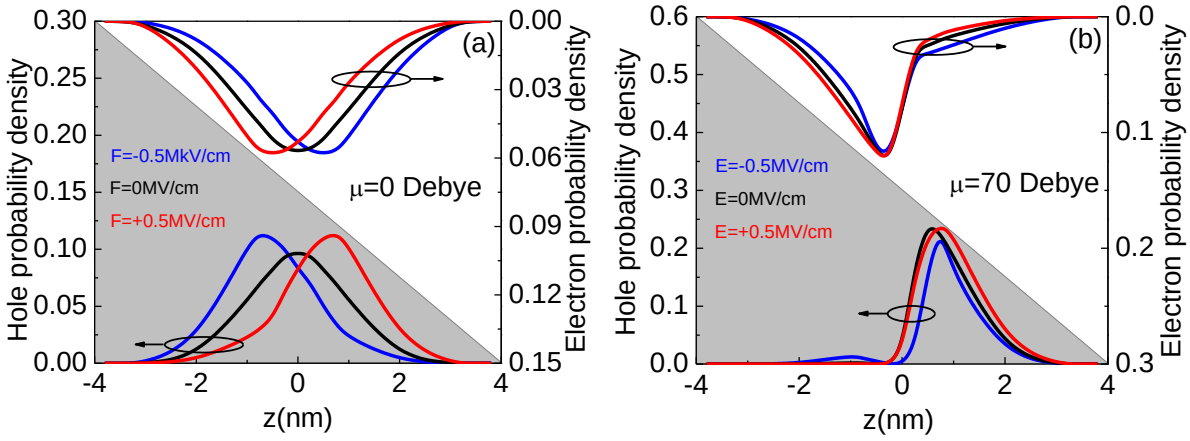

Figure 8. Electron and heavy-hole probability density distributions without (a) and with (b) intrinsic dipole moment under different electric field strength: -0.5MV/cm (blue), 0MV/cm (black) and 0.5MV/cm (red).

Table 1. Parameters derived from the fitting of $P(t_{on})$ and $P(t_{off})$ distributions from Figure 5 for groups QD(A) and QD(B) under zero and negative (-0.5 MV/cm) external bias.

Group	External bias (MV/cm)	m_{on}	$\Delta m_{on} = m_{on}(0) - m_{on}(-E)$	m_{off}	Δm_{off} $m_{off}(0) - m_{off}(-E)$
QD(A)	0	1.36	-0.17	1.36	0
	-0.5	1.53		1.36	
QD(B)	0	1.56	+0.27	1.80	0
	-0.5	1.29		1.86	

Table of Content

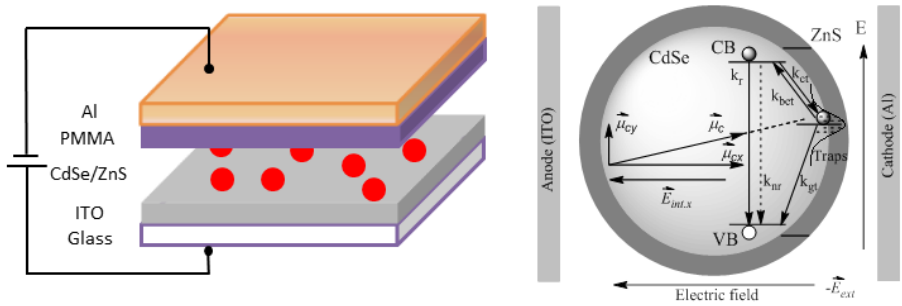

Single nanocrystal spectroscopy of CdSe/ZnS quantum dots under external electric field provides evidence of an intrinsic permanent dipole moment.